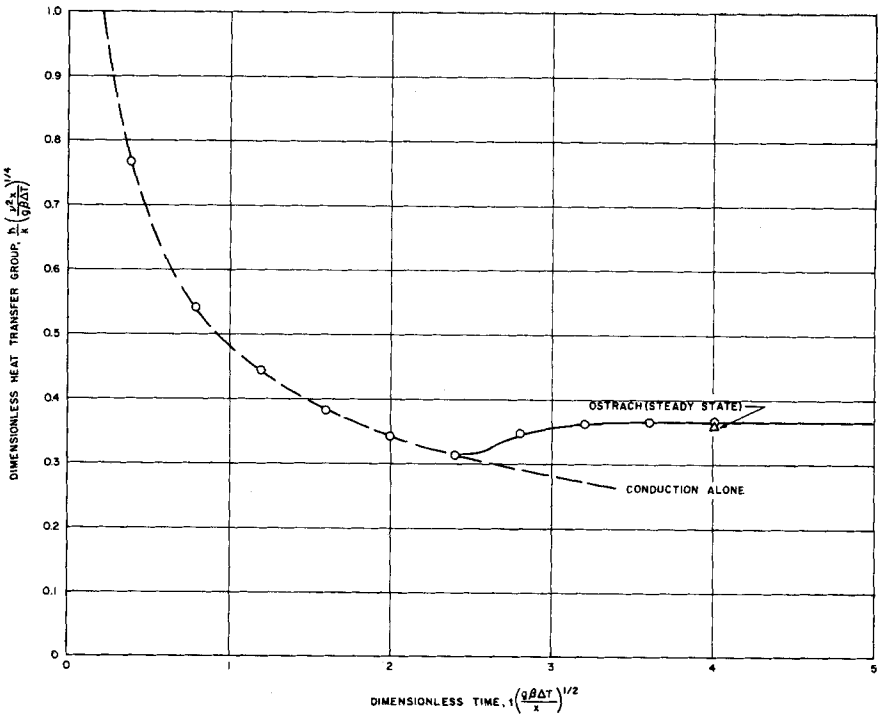

Fig. 6. Transient heat flux.

less the analytical solution for conduction alone and the numerical solution are indistinguishable; that is the solution for conduction alone is valid for most of the time required to approach the steady state value.

Siegel (2) estimated that the solution for conduction alone would be valid for $t(g\beta\Delta T/x)^{1/2} \leq 2.7$, which is in good agreement with the computed limit of 2.4. However his estimate of 7.1 for the dimensionless time required to reach steady state is about twice the value indicated in Figure 6. This latter value of course depends on the arbitrary choice of the fraction of the steady state value which is attained. When the dimensionless time equals 4.0, the heat transfer group is within 0.3% of the steady value. A dimensionless time of 7.0 is required to obtain agreement with the steady state to five significant figures.

The existence of a temporal minimum in the heat transfer coefficient has been noted previously. Klei (8) observed a minimum in his constant heat flux experiments, and both Siegel (5) and Gebhart (6) predicted one by analysis.

CONCLUSIONS

The results herein are apparently the first complete solution for transient free convection in any geometry.

The excellent agreement between the numerical solution and previous solutions for short times and the steady state gives credence to the results for intermediate times.

The existence of a temporal minimum in the heat transfer coefficient is confirmed. The velocity and temperature at all points go through corresponding maximum values.

The time required for the heat transfer coefficient to approach its steady state value is somewhat less than the time predicted by Siegel (5).

Dimensional analysis indicates that the numerical solution presented herein is reliable only for $N_{Pr} = 0.733$ but is applicable for any fluid properties or temperatures within this restriction, insofar as the idealizations in the theoretical model are valid.

NOTATION

g = acceleration due to gravity
h = local heat transfer coefficient
k = thermal conductivity of fluid
N_{Pr} = ν/α = Prandtl number of fluid
t = time
T = temperature
T_i = initial temperature of fluid
T_w = temperature of plate
u = component of velocity in vertical direction
U = $u/(\nu g\beta\Delta T)^{1/3}$
v = component of velocity in horizontal direction
V = $v/(\nu g\beta\Delta T)^{1/3}$
x = vertical distance above bottom of plate
X = $x(g\beta\Delta T/\nu^2)^{1/3}$
y = horizontal distance from plate
Y = $y(g\beta\Delta T/\nu^2)^{1/3}$

Greek Letters

α = thermal diffusivity of fluid
β = coefficient in equation of state of fluid (see reference 7)
ΔT = $T_w - T_i$
ν = kinematic viscosity of fluid
ϕ = $(T - T_i)/\Delta T$
ρ = density of fluid
τ = $t(g\beta\Delta T)^{2/3}/\nu^{1/3}$

Part II. The Region Inside a Horizontal Cylinder

Numerical values are presented for the transient and steady state temperature field, velocity field, and local heat transfer coefficient within an infinitely long, horizontal cylinder with vertical halves of the wall at different uniform temperatures. Despite the many idealizations in the theoretical model the solution agrees reasonably well with previous experimental data for the steady state. The steady state solutions encompass a greater range of N_{Gr} and N_{Pr} than the experimental data, and the asymptotic solution for large N_{Gr} is found to be a reasonable approximation for a wide range of N_{Pr} and N_{Gr}, permitting generalization of the numerical results. The transient motion is found to be quite complex, and the local heat transfer coefficients are found to decrease to a minimum and then go through a maximum before attaining a steady value.

A numerical solution for transient, free convection in the unconfined region adjacent to an isothermal, vertical plate was presented in Part I of this paper. The region confined by an infinitely long, horizontal cylinder with vertical halves at different uniform

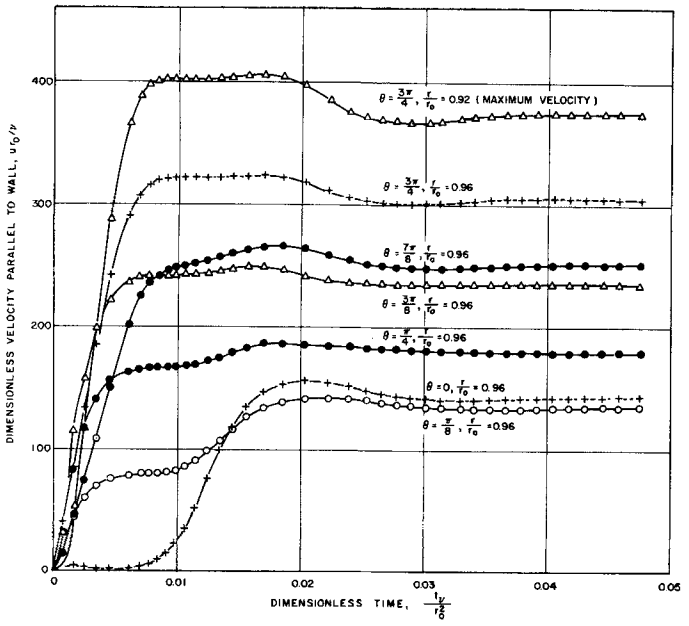

Fig. 1. Transient velocities.

TABLE 1. SUMMARY OF STEADY STATE CALCULATIONS

	Solution			
	No. 1	No. 2	No. 3	No. 4
$N_{Gr} = g\beta r_o^3 \Delta T/\nu^2$	6.15 by 10^6	4.5 by 10^4	1.0 by 10^7	6.15 by 10^6
$N_{Pr} = \nu/\alpha$	0.7	0.7	0.7	10.0
$(N_{Gr} \cdot N_{Pr})^{1/4} = (g\beta r_o^3 \Delta T/\nu\alpha)^{1/4}$	25.6	13.32	51.4	49.8
$N_{Nu_m} = h_m D/k$	9.43	4.56	18.34	16.29
$(h_m/k)(\alpha\nu r_o/g\beta\Delta T)^{1/4}$	0.184	0.171	0.178	0.163

temperatures was selected for further calculations as a problem for which no solution is available but for which steady state, experimental data exist. The experiments of Martini and Churchill (9) appear to be the only ones for natural convection in an enclosed space in which both the velocity and temperature fields were measured.

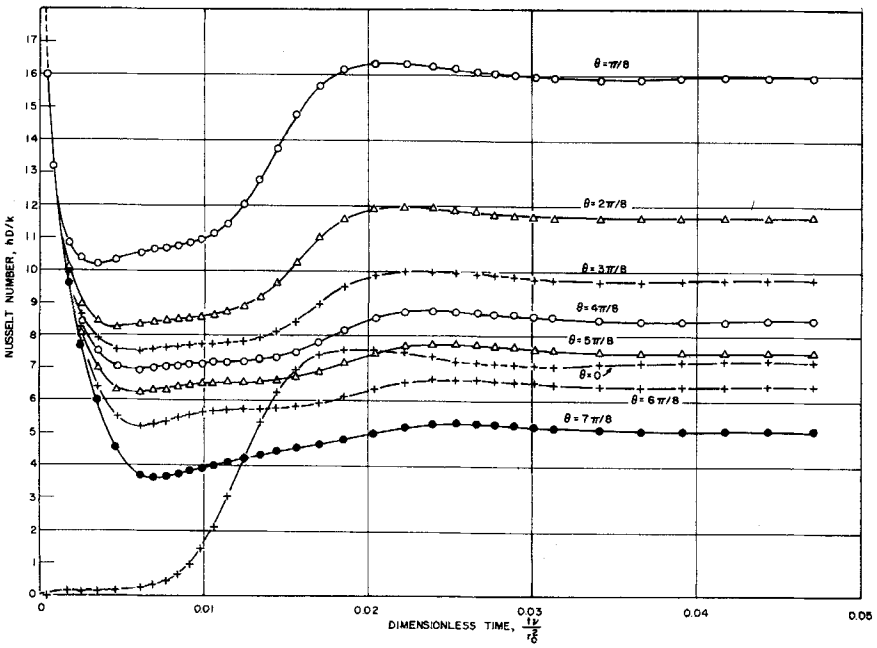

Fig. 2. Transient Nusselt numbers.

The partial differential equations describing the conservation of mass, momentum, and energy within the fluid were solved in time-dependent form by finite difference methods on an IBM-704 computer. The method of solution is described in detail in references *1* and *2*.

For the transient calculations a fluid initially at rest at a uniform temperature equal to the average of the opposing wall temperatures was arbitrarily selected. The steady state results are of course independent of the choice of an initial condition.

MATHEMATICAL DESCRIPTION

The conservation of momentum, energy, and mass in the fluid within the cylinder is approximately described by the following dimensionless equations:

$$\frac{\partial U}{\partial \tau} + \frac{U}{R}\frac{\partial U}{\partial \theta} + V\frac{\partial U}{\partial R} = N_{Gr}\,\phi \sin\theta + \frac{\partial}{\partial R}\left(\frac{1}{R}\frac{\partial UR}{\partial R}\right) + \frac{1}{R^2}\frac{\partial^2 U}{\partial \theta^2} \quad (1)$$

$$\frac{\partial \phi}{\partial \tau} + \frac{U}{R}\frac{\partial \phi}{\partial \theta} + V\frac{\partial \phi}{\partial R} = \frac{1}{N_{Pr}}\left[\frac{1}{R}\frac{\partial}{\partial R}\left(R\frac{\partial \phi}{\partial R}\right) + \frac{1}{R^2}\frac{\partial^2 \phi}{\partial \theta^2}\right] \quad (2)$$

$$\frac{\partial (RV)}{\partial R} + \frac{\partial U}{\partial \theta} = 0 \quad (3)$$

The idealizations in this representation are discussed in reference *2*. The principal assumptions are large N_{Gr} and $\beta\Delta T << 1$.

The chosen boundary and initial conditions are

$U = V = 0, \phi = 1/2$
at $R = 1, 0 \leq \theta \leq \pi$
$U = V = 0, \phi = -1/2$
at $R = 1, \pi \leq \theta \leq 2\pi$
$U = V = \phi = 0$
at $\tau = 0$

and

$$U(R, \theta, \tau) = U(R, \theta + \pi, \tau)$$
$$V(R, \theta, \tau) = V(R, \theta + \pi, \tau)$$
$$\phi(R, \theta, \tau) = -\phi(R, \theta + \pi, \tau)$$

THE TRANSIENT SOLUTION

A complete transient solution for a fluid initially at rest and at a uniform temperature was computed for $N_{Gr} = 6.15 \times 10^6$ and $N_{Pr} = 0.7$. Eventually

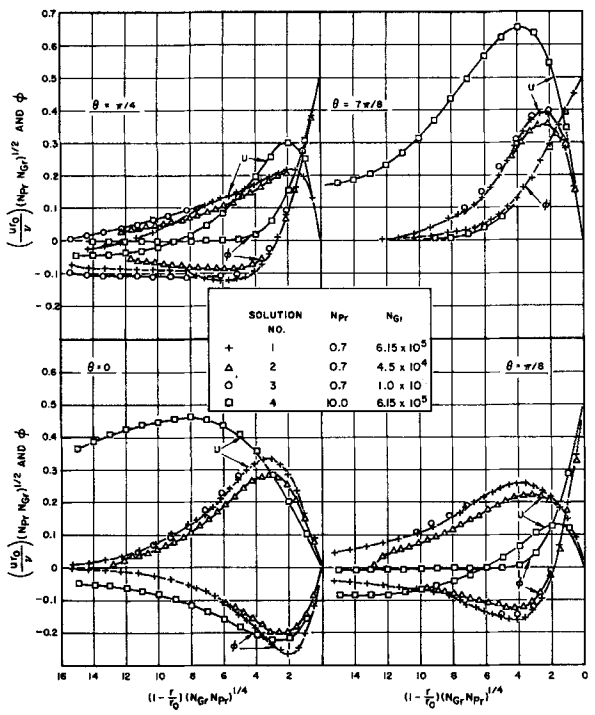

Fig. 3. Velocity and temperature profiles near the discontinuity in wall temperature.

a steady state is attained in which a thin layer of fluid circulates around the circumference of the cylinder, while the inner core of the fluid is nearly isothermal and motionless.

Figure 1 shows the dimensionless velocity Ur_o/ν as a function of the dimensionless time $t\nu/r_o^2$ at various positions. The behavior with time is quite complex. The velocity along the radii $\theta = 0$ and $\theta = \pi$ remains very low, while the velocity along other radii increases to a pseudosteady state. The velocity along $\theta = 0$ and $\theta = \pi$ then increases causing adjustments in the velocities elsewhere. This behavior may be explained by the fact that the buoyant force on the fluid near the boundary along the radii $\theta = 0$ and $\theta = \pi$ acts perpendicular to the boundary but has a tangential component elsewhere. Eventually a velocity across these vertical rays is established by momentum.

Figure 2 shows the variation of N_{Nu} with time at various positions around the cylinder wall. N_{Nu} appears to attain steady values somewhat sooner than the velocity. This behavior is characteristic of all the calculations; that is N_{Nu} is insensitive to small variations in the velocity field. At time zero the boundary temperature changes discontinuously everywhere except at $\theta = 0$ and $\theta = \pi$. At these two positions the initial value of N_{Nu} is zero; elsewhere the initial value of N_{Nu} is infinite.

STEADY STATE RESULTS

Dimensional analysis of Equations (1), (2), and (3) for the steady state, asymptotic case of $N_{Gr} \to \infty$ with $N_{Pr} \neq 0$ indicates that $U(N_{Pr}/N_{Gr})^{1/2}$, $V(N_{Pr}^2/N_{Gr})^{1/4}$, and ϕ depend only on θ, $(1 - r/r_o)\ (N_{Gr}N_{Pr})^{1/4}$, and N_{Pr}, and that $N_{Nu}/(N_{Gr}N_{Pr})^{1/4}$ depends only on θ and N_{Pr}. For $N_{Pr} \to \infty$ as well the dependence on N_{Pr} drops out. The indicated behavior for these limiting cases proves to be very useful in interpreting and correlating the computed values for finite N_{Gr} and N_{Pr}. The method of dimensional analysis used here is described in reference 7, and the details of the analysis for this problem are given in reference 2.

In addition to the steady state solution provided by the transient calculations, steady state solutions were obtained for three conditions by starting with estimates of the steady tempera-

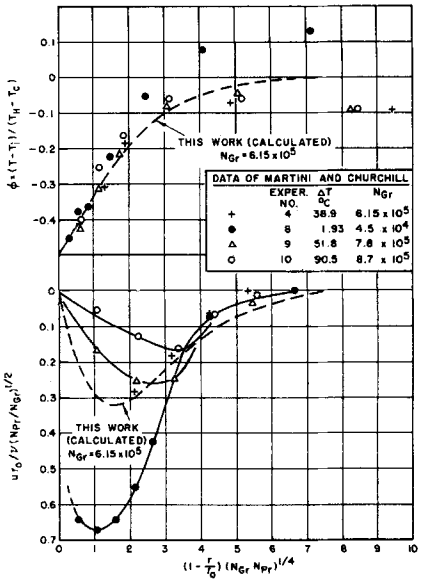

Fig. 5. Comparison of calculated and measured temperatures and velocities along $\theta = 3\pi/2$.

ture and velocity fields thus reducing the machine time. The conditions and results for the four cases are summarized in Table 1. A coarser grid was used for solution number 2 than for the other three. Solution number 3 for $N_{Gr} = 10^7$ is presumed to approximate the asymptotic case of $N_{Gr} \to \infty$.

The velocity and temperature fields are illustrated for four radii in Figure 3. Where the values are coincident only the symbol for solution number 1 is shown. The profiles for the three solutions with $N_{Pr} = 0.7$ are brought together quite well by the use of the composite variables suggested by the dimensional analysis. The profiles for solution number 2 deviate a maximum of 15% from the profiles for solution number 3 in the region of maximum velocity, and much less near the wall $(R = 1)$. This deviation is undoubtedly in part due to the use of a coarser grid. The velocity field for solution number 4, which is for $N_{Pr} = 10.0$, deviates considerably from the others. The fluid with the larger N_{Pr} accelerates and decelerates more than the fluid with lower N_{Pr} while travers-

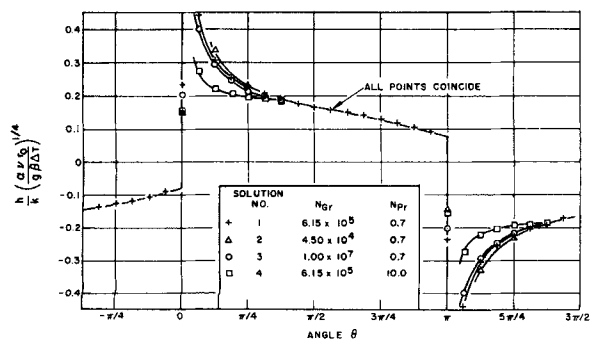

Fig. 4. Local heat transfer rates.

ing the hot and cold walls, respectively. This behavior is in accordance with the analyses in references 2 and *10* which demonstrate that the relative importance of the inertial terms in the partial differential equations depends on N_{Pr}.

The temperature fields for the fluids of different N_{Pr} are in better agreement than the velocity profiles. Along the ray $\theta = 7\pi/8$ the temperatures almost coincide, but an appreciable difference exists near the bottom of the cylinder.

The local heat transfer coefficient around the wall is plotted in Figure 4. The dimensionless heat transfer group $(h/k)\,(\alpha\nu r_o/g\beta\Delta T)^{1/4}$ varies only slightly with N_{Gr} and only near the discontinuities in wall temperature with N_{Pr}.

The mean Nusselt number is observed in Table 1 to increase with both N_{Pr} and N_{Gr}, but the group $(h_m/k)/(\alpha\nu r_o/g\beta\Delta T)^{1/4}$ is almost invariant. The 4% decrease in this group as N_{Gr} is increased from 6.15×10^4 to 1.0×10^7 is presumed to be real, but the 4% deviation of solution number 2 below the asymptotic value of 0.178 is probably due to the difference in the grid used for the calculations. $(h_m/k)/(\alpha\nu r_o/g\beta\Delta T)^{1/4}$ decreases only from 0.184 to 0.163 as N_{Pr} is increased from 0.7 to 10.0 at $N_{Gr} = 6.15 \times 10^5$.

COMPARISONS WITH EXPERIMENTAL DATA

The calculated temperature and velocity profiles along the ray $\theta = 3\pi/2$ are plotted in Figure 5 together with the experimental data of Martini and Churchill (9). The calculated curves and the data for experiment number 4 (+ symbol) are for $N_{Gr} = 6.15 \times 10^5$ and $N_{Pr} = 0.7$. Experiment number 8 is for a lower ΔT and N_{Gr} and 9 and 10 for larger ΔT and N_{Gr}. The experimental values of N_{Pr} and N_{Gr} in Figure 5 are based on the average of the physical properties for the two sides of the cylinder because N_{Gr} based on the cold-side properties was as great as nineteen times that based on hot-side properties.

The model for the calculations assumed invariant properties; therefore deviations from the experimental values at large temperature differences would be expected. On the other hand the model is presumed to be valid only for large N_{Gr} so deviations would also be expected at very small temperature differences.

In view of these considerations the observed agreement with experiment number 4 is surprisingly good. The deviations for the larger and smaller temperature differences are greater than indicated by the calculations for the effect of N_{Gr} and are presumed to be due instead to the differences mentioned above between the model and the experiments.

The thirteen experimental values of the mean heat transfer coefficient for the hot side of the cylinder and the calculated values are compared in Figure 6. The upper portion of the figure is in the conventional form of N_{Nu} vs. $N_{Gr} \cdot N_{Pr}$, but the use of an arithmetic scale for the ordinate displays absolute rather than percentage deviations and thus emphasizes the scatter. The lower portion of the figure is in the more concise and critical form suggested by dimensional analysis. The straight line in both portions represents the asymptotic solution (h_m/k)

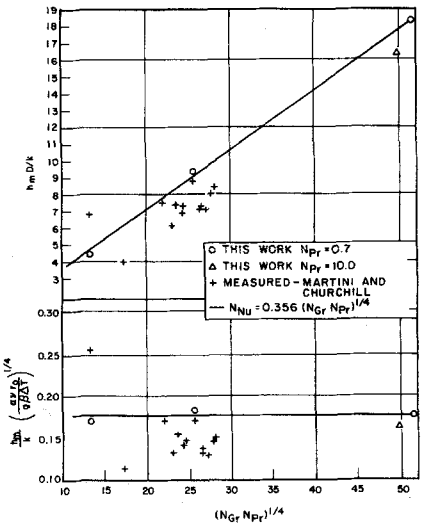

Fig. 6. Comparison of overall heat transfer results.

$(\alpha\nu r_o/g\beta\Delta T)^{1/4} = 0.178$ or $N_{Nu} \cdot N_{Gr}^{-1/4} \cdot N_{Pr}^{-1/4} = 0.356$.

The calculations were for a step in wall temperature at the top and bottom of the cylinder, while in the experiments this discontinuity was approximated by a steep gradient across a thin strip of insulation. The effective temperature difference for experiments would therefore be expected to be somewhat less than the nominal difference, and the experimental heat transfer coefficient would presumably be reduced. This may account in part for the presence of all but one experimental point below the line representing the calculations. The one experimental point above the line is experiment number 8 in which the temperature difference was less than 2°C. A possible reason for the discrepancies in the velocity and temperature profiles for this experiment was mentioned above. However the great uncertainty in the determination of the heat transfer coefficient from the temperature gradient in this particular experiment is a more likely explanation for the deviation of the coefficient.

SUMMARY AND CONCLUSIONS

The numerical solution agrees reasonably well with the steady state measurements of Martini and Churchill despite several obvious differences in the mathematical model and the experimental system. It therefore appears that numerical integration of the partial differential equations for the conservation of mass, momentum, and energy is a practical and reliable method of a priori prediction of natural convection in confined as well as unconfined fluids.

The idealizations in the theoretical model were made for simplicity rather than because of necessity. The pattern of the deviations suggests that the discrepancies could readily be reduced by modification of the model. Such modifications as variable viscosity would not greatly complicate the calculations but would yield a specific solution for a particular fluid, etc.

The strength and utility of the method of dimensional analysis described in reference 7 for guiding calculations and interpreting and correlating experimental or numerical results is clearly demonstrated by this investigation.

The transient motion inside the cylinder is shown to be quite complex but can be explained qualitatively on physical grounds. Except at the two discontinuities in wall temperature the local heat transfer coefficient decreases from infinity to a minimum, increases to a maximum, and finally decreases slightly to the steady state value.

The steady state values encompass a greater range of N_{Gr} and N_{Pr} than the experimental values of Martini and Churchill, and the asymptotic solution for large N_{Gr} appears to be a good approximation for a wide range of values of N_{Gr} and N_{Pr}.

ACKNOWLEDGMENT

The assistance and cooperation of the staff of the University of Michigan Computing Center are gratefully acknowledged. Financial support was provided J. D. Hellums by the Bendix Aviation Corporation Fellowship.

NOTATION

D = diameter of the cylinder
g = acceleration due to gravity
h = local heat transfer coefficient $= q/(T_H - T_c)$
h_m = overall heat transfer coefficient $= \frac{1}{\pi}\int_o^\pi h\, d\theta$
k = thermal conductivity of fluid
N_{Gr} = Grashof number $= g\beta\Delta T r_o^3/\nu^2$

(Continued on page 719)

dense phase flow behavior of gas fluidized solids in changing area flow behavior of gas fluidized solids in changing area flow sections is presented. A dimensionless process diagram is described.

Computer Program Abstracts

Readers of the *A.I.Ch.E. Journal* who are interested in programming for machine computation of chemical engineering problems will find in each issue of *Chemical Engineering Progress* abstracts of programs submitted by companies in the chemical process industries. Collected by the Machine Computation Committee of the A.I.Ch.E., these programs will be published as manuals where sufficient interest is indicated. The following abstracts have appeared this year:
CEP (October, 1962) p. 84

Calibration of Inclined Tanks with Dished Heads (101)

Analytical Solution of Fourth Order Equations (102)

(Continued from page 695)

N_{Nu} = Nusselt number = $2hr_o/k$
N_{Pr} = Prandtl number = ν/α
q = local heat flux density on cylinder wall
r = radial distance
r_o = radius of the cylinder
R = r/r_o
t = time
T = temperature
T_H = temperature of hot side of cylinder
T_c = temperature of cold side of cylinder
T_i = initial temperature = $(T_H + T_c)/2$
u = velocity component in the θ direction
U = ur_o/ν
v = velocity components in the radial direction
V = vr_o/ν

Greek Letters

α = thermal diffusivity of fluid
β = coefficient in equation of state (see reference 7) = $1/T_i$
ΔT = $T_H - T_c$
ν = kinematic viscosity of fluid
ϕ = $(T - T_i)/\Delta T$
τ = $t\nu/r_o^2$
θ = angle measured from bottom of cylinder through hot wall

LITERATURE CITED

1. Hellums, J. D., and S. W. Churchill, Proceedings of the International Heat Transfer Conference 1961, to be published.
2. Hellums, J. D., Ph.D. thesis, Univ. of Michigan, Ann Arbor, Michigan (1960).
3. Schmidt, E. H. W., and W. Beckmann, *Tech. Mech. u. Thermodynam.*, **1**, 341, 391 (1930).
4. Ostrach, Simon, *Natl. Advisory Comm. Aeronaut. Rept. 1111* (1953).
5. Siegel, Robert, *Trans. Am. Soc. Mech. Engrs.*, **80**, 347 (1958).
6. Gebhart, Benjamin, *J. Heat Transfer*, **83**, Series C, No. 1, 61 (1961).
7. Hellums, J. D., and S. W. Churchill, *Chem. Eng. Progr. Symposium Ser. No. 32*, **57**, 75 (1961).
8. Klei, H. E., M.S. thesis, Mass. Inst. Technol., Cambridge, Massachusetts (1957).
9. Martini, W. R., and S. W. Churchill, *A.I.Ch.E. Journal*, **6**, 251 (1960).
10. Morgan, G. E., and W. H. Warner, *J. Aeronaut. Sci.*, **23**, 937 (1956).

Manuscript received April 25, 1961; revision received June 6, 1962; paper accepted June 8, 1962. Paper presented at A.I.Ch.E. Cleveland meeting.